Stochino, F., Majumder, A., Kanagaraj, B., Sara, N., Serra, A., & Mistretta, F. (2025). Combining experimental and computational approaches for post-fire safety assessment of RC warehouse. Proceedings of the Institution of Civil Engineers-Forensic Engineering, 178(3), 66-80.

https://doi.org/10.1680/jfoen.25.00027

Please cite this document as: Stochino, F., Majumder, A., Kanagaraj, B., Sara, N., Serra, A., & Mistretta, F. (2025). Combining experimental and computational approaches for post-fire safety assessment of RC warehouse. *Proceedings of the Institution of Civil Engineers-Forensic Engineering*, *178*(3), 66-*80*. *https://doi.org/10.1680/jfoen.25.00027*

Combining Experimental and Computational Approaches for Post-Fire Safety Assessment of RC Warehouse

Flavio Stochino[1*], Arnas Majumder[1] , Balamurali Kanagaraj[2], Nicola Sara[3] , Alessio Serra[4], Fausto Mistretta[1]

[1]Department of Civil Environmental Engineering and Architecture, University of Cagliari, Cagliari, Italy

[2]Division of Civil Engineering, Karunya Institute of Technology and Sciences, Coimbatore, India

[3]CVS Associati, Sassari, Italy

[4] Impresa di Costruzioni Ing. Raffaello Pellegrini srl, Cagliari, Italy

** Corresponding author: fstochino@unica.it*

Abstract

This paper addresses the critical need for accurate post-fire assessment of reinforced concrete (RC) warehouses, where fire-induced damage can compromise structural safety and repair strategies. Traditional visual inspection and conservative design assumptions often fail to capture the true extent of degradation, especially under realistic fire scenarios. To overcome these limitations, we present a combined Computational Fluid Dynamics (CFD) and Finite Element (FE) framework that simulates the warehouse fire environment, estimates thermal exposure, and evaluates its impact on the structural response and residual capacity of damaged RC elements. Experimental diagnostics — including laser scanning, non-destructive testing, and material sampling — were conducted to calibrate the models and quantify damage. Our findings highlight that the proposed methodology enables a more reliable identification of severely compromised components, supports targeted and cost-effective retrofitting interventions, and offers practical guidance for improving resilience in similar structures. This work advances performance-based fire engineering by demonstrating a validated and holistic assessment strategy that can inform reconstruction decisions and enhance fire safety practices in industrial buildings.

1. Introduction

Fire remains one of the most critical hazards to structural safety and integrity, with a non-negligible probability of occurrence in various real-world scenarios. It is categorized as an extreme loading event, on par with blasts and impacts, as specified in several international structural design codes and standards, due to the potential severity of its effects (Ma *et al.*, 2025). In many incidents, fires are either triggered by or lead to explosions, which subject structures to compounded thermal and mechanical loads that push materials beyond their conventional performance limits (Stochino, 2016) (Pinna *et al.*, 2025) (Chen *et al.*, 2024) (Pinna and Stochino, 2025)

Among the most widely used structural materials, Reinforced Concrete (RC) is particularly sensitive to high-temperature exposure. Its mechanical properties, such as compressive strength,

Please cite this document as: Stochino, F., Majumder, A., Kanagaraj, B., Sara, N., Serra, A., & Mistretta, F. (2025). Combining experimental and computational approaches for post-fire safety assessment of RC warehouse. *Proceedings of the Institution of Civil Engineers-Forensic Engineering*, *178*(3), 66-*80*. *https://doi.org/10.1680/jfoen.25.00027*

stiffness, and bond strength, deteriorate significantly with temperature rise (Çelik and Urtekin, 2025) (Jiao *et al.*, 2014) (Saeed and Al-Ahmed, 2025). To capture this behavior, a variety of thermo-mechanical models have been developed and validated against experimental data (Li *et al.*, 2004). However, accurate structural assessment after a fire event demands more than just knowledge of material degradation, as well as requires reconstructing the temperature-time history and understanding the evolution of stress and strain fields during and after exposure (Osman *et al.*, 2017) (La Scala, Loprieno, *et al.*, 2024).

Therefore, the importance of performance-based fire engineering is gaining momentum, in which the prime objective is to evaluate structural performance under realistic fire conditions rather than just following prescriptive regulations. Using well-documented case studies can improve this method by giving accurate information about temperature changes and how structures react (Gernay, 2024).

In this context, modern computational tools play a pivotal role. Computational Mechanics, particularly Finite Element (FE) analysis and Computational Fluid Dynamics (CFD), offers robust and flexible methods to simulate the highly nonlinear and time-dependent behavior of materials and structures under fire conditions (La Scala *et al.*, 2023) (La Scala, Śliwa-Wieczorek, *et al.*, 2024).

CFD (McGrattan and Miles, 2016), which centers on the numerical solution of the Navier-Stokes equations (Chorin, 1968), is a powerful tool for simulating the complex behavior of fluids and gases under a wide range of physical conditions. In the context of fire engineering, CFD enables highly detailed modeling of key phenomena such as heat transfer through convection and radiation, flame propagation, smoke movement, and fluid-structure interactions (Wen, 2024). These processes are inherently nonlinear and often occur simultaneously in highly dynamic and geometrically complex environments, such as multi-room buildings, tunnels, or industrial facilities. Analytical solutions to the Navier-Stokes equations are only feasible for very simple and idealized problems due to the nonlinear nature of the equations and the wide range of boundary conditions encountered in real-world scenarios.

Fires create turbulent airflow and have material properties that change with temperature. The changing conditions in fire scenarios make analytical solutions difficult, so CFD-based numerical methods are essential for accurately modeling the interactions between fire and structural responses (Maragkos and Beji, 2021).

Recent advancements in post-fire safety assessment of reinforced concrete (RC) structures demonstrate the effective integration of experimental and computational approaches.

(Khan *et al.*, 2021) reviews the evolution and current state of fire models for structural fire assessment, focusing on gas temperature predictions and their role as “loads” on structures. It also explores recent advances in CFD-FEM coupling for more realistic fire-structure interaction simulations. A new methodology for the mechanical and thermal design of composite slabs under fire is proposed in (Bolina and Rodrigues, 2022) following a thorough numerical modelling of this problem. These studies highlight the importance of combining experimental validation with advanced computational models to accurately assess and enhance the post-fire safety of RC structures.

In addition, many interesting case study of post fire assessment can be found in recent literature: (Raposo *et al.*, 2025) investigates the causes of a house fire in Arganil, Portugal, identifying construction flaws, materials, and heat sources to prevent similar incidents in the future. A comprehensive review on fire damage assessment of reinforced concrete structures is presented in (Qin *et al.*, 2022) with specific attention to damage assessment measures for RC structures.

Despite the growing adoption of computational techniques for structural fire engineering, a significant research gap persists in the integration of experimental diagnostics with advanced numerical modeling (Yan *et al.*, 2024) for real-world post-fire assessments. Most existing studies either focus on idealized laboratory scenarios or adopt oversimplified thermal boundary conditions in structural models, failing to reflect the complexity and heterogeneity of actual fire events in large-scale RC structures. Furthermore, limited case studies combine in situ material testing, microstructural analyses, and CFD-informed finite element simulations in a unified framework. This paper addresses this gap by presenting a comprehensive investigation of a fire-damaged RC warehouse, coupling non-destructive and destructive testing, mineralogical and thermal analysis, and high-fidelity CFD and FE modeling. The aim is to develop a practical methodology for reliable post-fire safety assessments and to inform effective retrofitting strategies based on realistic thermal and mechanical behavior.

Indeed, in this study, a coupled approach combining CFD and Finite Element (FE) analysis is applied to a real-world case involving a reinforced concrete (RC) structure that sustained significant damage due to fire. The CFD model is used to simulate the thermal environment during the fire, including temperature distribution and heat fluxes on the surfaces of structural elements. This thermal data is then used as input for the FE analysis, which models the structural response of the RC components, taking into account temperature-dependent degradation in material properties such as strength and stiffness. By integrating these two advanced computational techniques, this paper proposes a coupled simulation framework to assess thermal exposure and structural degradation in fire-damaged buildings, enhancing our understanding of fire-induced failures and aiding in performance-based fire design. Ultimately, the insights gained contribute to more informed decision-making in post-fire structural assessments and promote the design of safer, more resilient built environments.

This paper is structured as follows**:** after this brief introduction, Section 2 provides comprehensive data on the building's construction. Section 3 offers a review of the fire impact. Section 4 discusses the findings derived from Computational Fluid Dynamics (CFD) and Finite Element (FE) modeling. Finally, Section 5 concludes the paper with key remarks and insights.

Please cite this document as: Stochino, F., Majumder, A., Kanagaraj, B., Sara, N., Serra, A., & Mistretta, F. (2025). Combining experimental and computational approaches for post-fire safety assessment of RC warehouse. *Proceedings of the Institution of Civil Engineers-Forensic Engineering*, *178*(3), 66-*80*. *https://doi.org/10.1680/jfoen.25.00027*

2. Basic data on the construction

The structure under investigation is a precast prestressed reinforced concrete warehouse built in 2010 in the outskirts of Cagliari (Italy). It consists of a single building with a footprint of approximately 60 m × 40 m (of total surface area of 2400 m²) and a height slightly over 11 m. The ground floor has a clear ceiling height of about 6 m and is divided into three compartments of approximately 800 m² each. Whereas the first floor is an open space with a total surface area of 2400 m², with a clear ceiling height of approximately 3.50 m. Notably, the load-bearing structure comprises (1) columns made of vibrated reinforced concrete with a rectangular cross-section. Three types can be identified based on their dimensions : (a) 0.68 x 0.50 m, (b) 0.90 x 0.50 m, and (c) 0.50 x 0.50 m; (2) Rectangular prestressed concrete beams of type TR, with approx. 0.80 m × 0.90 m (see Figure 1. a); (3) Ribbed “omega” beams approximately 2.55 m wide (see Figure 1. b).

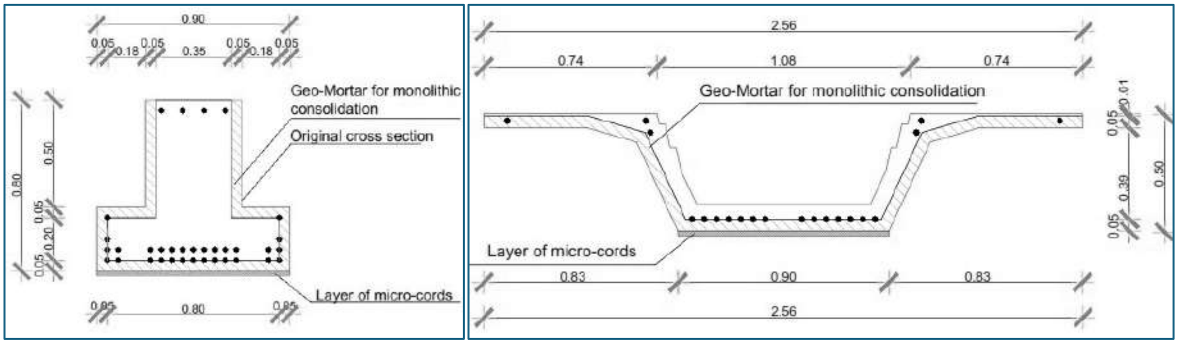

(a) *(b)*

Figure 1. The load-bearing structures: (a) Rectangular prestressed concrete beams of type TR

On the other hand, the roofing is made using TH 120 type pre-stressed reinforced concrete beams with Aliant 2 type elements, see Figure 2 (a).

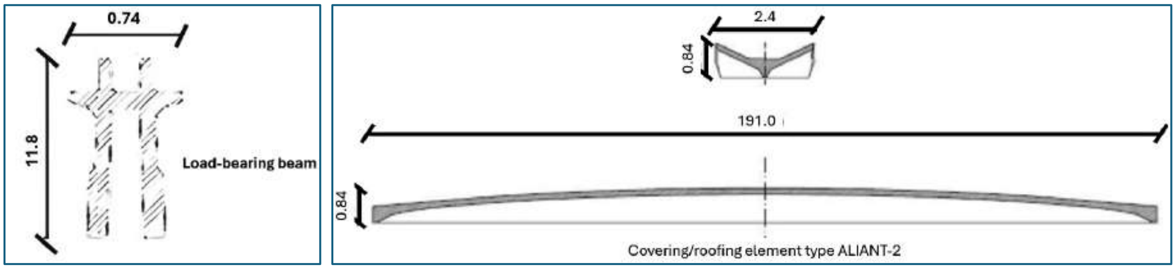

(a) *(b)*

Figure 2. (a) TH 120 beam, and (b)covering element of type Aliant 2

The floor system consists of precast panels joined to supporting beams through a cast-in-place concrete slab. It is designed to support a total load of 850 kg/m², comprising 400 kg/m² of live load and 200 kg/m² of dead load, whereas 250 kg/m² is the load of the 10 cm thick reinforced concrete slab. The vertical enclosure comprises panels anchored at the base to the foundations or portal frames, and at the top to the perimeter beams. This configuration enables the transfer of horizontal

Please cite this document as: Stochino, F., Majumder, A., Kanagaraj, B., Sara, N., Serra, A., & Mistretta, F. (2025). Combining experimental and computational approaches for post-fire safety assessment of RC warehouse. *Proceedings of the Institution of Civil Engineers-Forensic Engineering*, *178*(3), 66-*80*. *https://doi.org/10.1680/jfoen.25.00027*

forces while allowing for longitudinal movement, thereby preventing the transmission of vertical loads.

According to the original design, characteristic compressive concrete strength is 46 N/mm^2, while reinforcement bars are characterized by a yielding strength of 430 N/mm^2 and a tensile strength of 540 N/mm^2 in the case of a diameter smaller than 12 mm; otherwise yielding strength is 430 N/mm^2 and tensile strength 480 N/mm^2. Moreover, prestressing tendons of the beams are characterized by a diameter of 3/8" (9.5 mm) and 1⁄2" (12.7 mm); their tensile strength is 1860 N/mm^2. More information about the structure characteristics can be found in (Stochino *et al.*, 2017a).

On the evening of November 16, 2013, a fire broke out on the ground floor, causing significant structural damage, as shown in *Figure 3*. Notably, the fire was contained to the central area of the ground floor and did not extend to other parts of the building (see *Figure 4*).

(a) *(b)*

Figure 3. Warehouse (a) outside view, and (b) inside view.

Please cite this document as: Stochino, F., Majumder, A., Kanagaraj, B., Sara, N., Serra, A., & Mistretta, F. (2025). Combining experimental and computational approaches for post-fire safety assessment of RC warehouse. *Proceedings of the Institution of Civil Engineers-Forensic Engineering*, *178*(3), 66-*80*. *https://doi.org/10.1680/jfoen.25.00027*

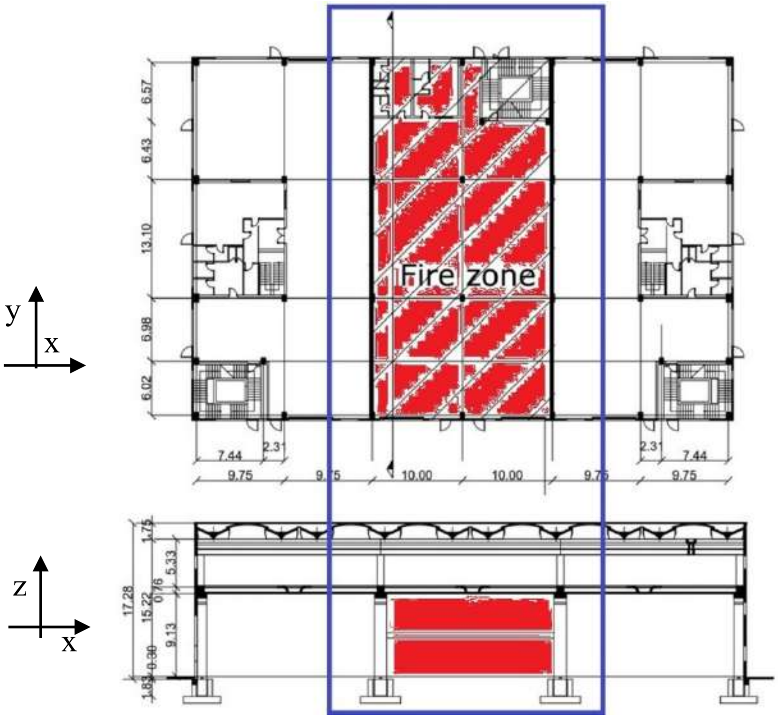

Figure 4. Primary Fire-Damaged Area in the Warehouse.

The presence of fire-resistant partition walls prevented the fire that broke out in one compartment from spreading to the others. The focus was therefore placed solely on the compartment affected by the flames. The fire completely destroyed both the interior spaces and the systems within the affected compartment, while the exterior facade shows no visible or apparent damage. The large amount of combustible material in the warehouse led to the fire's rapid development and swift spread. The damage was first analyzed in the study, and the related data were recorded to assess the degree of structural degradation. Based on the analyses carried out, it was concluded that although the damage caused by the fire was severe, with appropriate restoration work, it is possible to return the structure to its previous condition.

3. Fire Impact Review

3.1. Fire-induced destruction

After the fire, a substantial amount of debris was observed across almost the entire floor area. This debris consisted primarily of fragmented concrete, remnants of steel shelving units, charred wooden pallet pieces, and other fire-generated residues (*Figure 5*). The distribution and quantity of the debris suggest an intense fire that was localized in certain areas, causing widespread disintegration of both non-structural and structural elements, see *Figure 5*.

Please cite this document as: Stochino, F., Majumder, A., Kanagaraj, B., Sara, N., Serra, A., & Mistretta, F. (2025). Combining experimental and computational approaches for post-fire safety assessment of RC warehouse. *Proceedings of the Institution of Civil Engineers-Forensic Engineering*, *178*(3), 66-*80*. *https://doi.org/10.1680/jfoen.25.00027*

(a) (b) (c)

Figure 5. Damages inside the warehouse: (a) overview, (b) column, (c) beam.

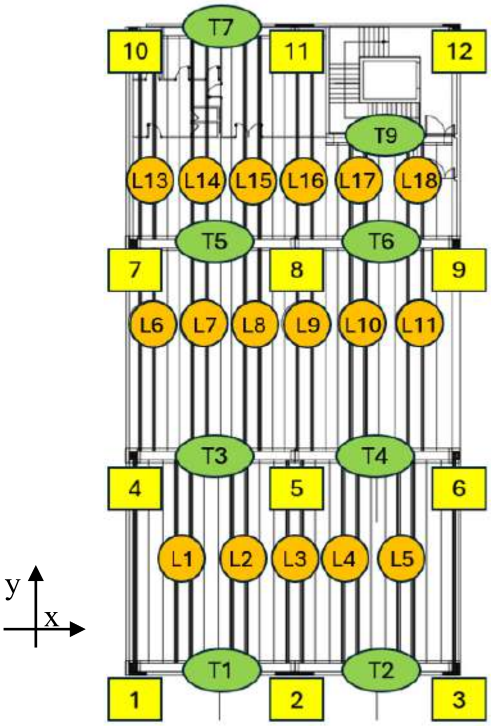

Figure 6. Plan view of the fire zone. T-shaped transversal beam are labelled with "T" while omega-shaped longitudinal beam are labelled with "L".

A detailed inspection of the structural frame revealed that the lateral columns identified as 4, 6, 7, and 9 (*Figure 6*) sustained the most extensive damage. Visual examination reveals that these columns were subjected to severe thermal exposure on one side, resulting in progressive material degradation inward toward the core. This pattern of damage suggests asymmetric heating, resulting in hollowing or loss of integrity on the fire-exposed faces (Figure 6).

Please cite this document as: Stochino, F., Majumder, A., Kanagaraj, B., Sara, N., Serra, A., & Mistretta, F. (2025). Combining experimental and computational approaches for post-fire safety assessment of RC warehouse. *Proceedings of the Institution of Civil Engineers-Forensic Engineering*, *178*(3), 66-*80*. *https://doi.org/10.1680/jfoen.25.00027*

In contrast, the perimeter columns 1, 2, 3, 10, 11, and 12 were located far from the central fire zone, therefore experienced considerably lower thermal exposure. Notably, their physical condition remains relatively intact, with no immediate signs of critical structural compromise.

The central columns, particularly columns 5 and 8, display surface characteristics indicative of high-temperature exposure. Their exteriors show significant roughness and a distinctive greyish-white coloration, a typical sign of surface dehydration and chemical changes in concrete under intense heat (Figure 6).

Regarding the horizontal structural elements, only the lower portions of the beams were directly exposed to the fire. The upper parts remained shielded by the concrete slab, which provided some level of thermal protection. However, in several beams, specifically T3, T4, T5, T6, L4, L5, L8, and L9 severe damage has been identified (Figure 6). These include substantial spalling of the concrete cover and partial debonding or exposure of the prestressing tendons, both of which can significantly compromise the load-bearing capacity and long-term durability of the beams.

These findings underscore the necessity for a comprehensive structural integrity assessment, potentially necessitating extensive repair or replacement of the most heavily affected components.

3.2. Analysis of Material Fatigue and Maximum Thermal Exposure

To determine the extent of mechanical degradation after a fire event, it is crucial to determine the maximum temperature reached during the fire (Meloni *et al.*, 2019). The authors have conducted a detailed geometric survey using laser scanning technology to identify permanent deformations caused by the fire. Subsequently, measurements of ultrasound wave velocity and rebound index were carried out on various structural elements. A load test was also performed on one of the most representative sections of the damaged structure. A number of cylindrical core samples were extracted from columns and slabs across different areas of the building, and a destructive compressive strength tests performed on these samples revealing that the average strength of fire-damaged precast concrete (from beams and columns) found to be about 30.5 N/mm², while the cast-in-place concrete (from slabs) exhibited an average strength of approximately 20.0 N/mm².

Further analyses including X-ray Diffraction (XRD), Differential Thermal Analysis (DTA), Optical and Scanning Electron Microscopy (SEM) (see Table 1 (Stochino *et al.*, 2017b)), and colorimetric tests (see Table 2) have been done, and these tests provided valuable insights into the temperatures experienced by the fire-exposed concrete. The conclusions were mainly drawn from the changes observed in the mineralogical composition and microstructure of the concrete materials. A comprehensive summary of the main findings is presented in Table 2 and Table 3. Notably Table 3 data have been used as a benchmark for the model development that will be presented in the next Sections.

Table 1. Key findings of non-destructive tests (Stochino *et al.*, 2017b).

Method	Purpose	Key Findings
X-ray Diffraction (XRD)	Identify mineralogical changes	- Undamaged: Calcite, dolomite, portlandite, ettringite present - Fire-damaged: Absence of portlandite (>500°C), formation of perovskite, spurrite - Decarbonation of calcite/dolomite (~700–900°C)
DTA & Thermogravimetry (TG)	Track thermal decomposition and estimate temperature	- Undamaged: Peaks at ~120°C (water), ~500°C (portlandite), ~750–950°C (carbonate decomposition) - Damaged: Loss of portlandite peak, high-temp decarbonation (~880°C), shifted dehydroxylation onset
Optical Microscopy (OM)	Assess microstructural damage and color change	- Undamaged: Compact, intact transition zone - Damaged: Microcracks (20–40 μm), reddening at 300–350°C, whitening at 600–900°C, surface pulverization (>700°C)
Scanning Electron Microscopy (SEM)	High-resolution imaging of microstructure	- Undamaged: Dense CSH, visible ettringite, no interfacial cracks - Damaged: Globular phases (melting), microcracks, aggregate-paste detachment, CSH degradation (>300°C)

Table 2. Colorimetric results (L, a* and b*) and mineralogical phases detected on samples collected in situ.*

Sample Series	**Sub-sample**	**Depth (cm)**	**Mineralogical Phases**	**L***	**a***	**b***	**Color Target**
Undamaged	—	0	E, Cal, Dol, P	62.08	0.03	2.72	CM
COL 4A	-a	0.5	Cal, Dol, P*	75.35	-0.61	5.25	CM
	-b	1.5	Cal, Dol	73.45	0.27	4.01	CM
	-c	2.5	Cal, Dol, P	61.23	0.47	4.35	CM
	-d	4.5	Cal, Dol, P	58.36	3.67	5.18	PBA
	-e	7.5	Cal, Dol, P	54.63	5.28	6.43	PBA
COL 5A	-1	6	Cal, Dol, P	61.84	0.85	4.35	CM
	-2	8	Cal, Dol, P	55.49	5.26	6.25	PBA
COL 5B	-1	0.5	Cal, Dol, P	70.55	0.21	4.25	CM
	-2	2	Cal, Dol, P	61.78	0.86	3.58	CM
	-3	2.7–4.5	Cal, Dol, P	55.49	5.13	6.43	PBA
COL 8A	-1	3	Cal, Dol, P	61.45	0.98	4.74	CM
	-2	5	Cal, Dol, P	57.54	5.36	6.42	PBA
COL 8B	—	0.5	Cal, Dol, P	55.49	5.8	6.62	PBA
COL 9A	—	9.7	Cal, Dol, P	57.4	4.25	6.47	PBA
COL 9B	—	7.8	Cal, Dol, P	55.12	4.84	5.98	PBA

Where, COL= column, Cal= Calcite, .CM = Cement Matrix, Dol = Dolomite, E= Ettringite, P=Portlandite, P*= relict or secondary Portlandite, PBA= Pinkish-beige aggregates.

Please cite this document as: Stochino, F., Majumder, A., Kanagaraj, B., Sara, N., Serra, A., & Mistretta, F. (2025). Combining experimental and computational approaches for post-fire safety assessment of RC warehouse. *Proceedings of the Institution of Civil Engineers-Forensic Engineering*, *178*(3), 66-*80*. *https://doi.org/10.1680/jfoen.25.00027*

Table 3. Synthesis of maximum temperature estimation detected on samples collected in situ.

Sample Series	**Est. Max Temp (°C)**
Undamaged	20
COL 4A	≈700
	>500
	≤500
	<500–400
	400–300
COL 5A	≤500
	400–300
COL 5B	>500
	≤500–400
	400–300
COL 8A	≤500
	400–300
COL 8B	—
COL 9A	400–300
COL 9B	400–300

Where, COL = column

4. Computational Fluid Dynamics (CFD) and Finite Element (FE) models

4.1. Solution Techniques

The fire scenario was modeled using the Fire Dynamics Simulator (FDS) [9], a computational fluid dynamics (CFD) tool designed to numerically solve the Navier–Stokes equations under conditions of low-speed, thermally driven flows such as those generated by smoke and heat during a fire. FDS approximates the partial differential equations governing the conservation of mass, energy, and momentum using second-order finite difference methods, solving them numerically across the mesh for each time step.

This study employs the Large Eddy Simulation (LES) approach as its solution strategy. LES focuses on resolving the larger turbulent structures influenced by the specific flow geometry, while modeling the smaller, more universal turbulence scales, which are considered independent of the particular features of the flow. The LES technique does not account for small-scale phenomena and instead relies on a simplified algorithm, based on a semi-empirical method developed by Smagorinsky (McGrattan, 2006). This approach directly incorporates the large-scale turbulence into the integration process, while the smaller turbulence structures are modeled.

The pyrolysis model in FDS utilizes a one-dimensional heat transfer equation to describe conduction through solid materials. This equation is solved using finite difference techniques.

For the combustion process, this study employs the combustion mixture-fraction method.

4.2. Case study through numerical simulation

Please cite this document as: Stochino, F., Majumder, A., Kanagaraj, B., Sara, N., Serra, A., & Mistretta, F. (2025). Combining experimental and computational approaches for post-fire safety assessment of RC warehouse. *Proceedings of the Institution of Civil Engineers-Forensic Engineering*, *178*(3), 66-*80*. *https://doi.org/10.1680/jfoen.25.00027*

The central compartment, illustrated in *Figure 7*, is treated as a single computational domain with a parallelepiped geometry. Its overall dimensions are 20.50 m (x-direction), 40.20 m (y-direction), and 6.80 m (z-direction), as shown in (*Figure 4* and *Figure 6*). The long sides are enclosed by REI 120-rated brick walls, while the short sides consist of prefabricated concrete panels with openings, also visible.

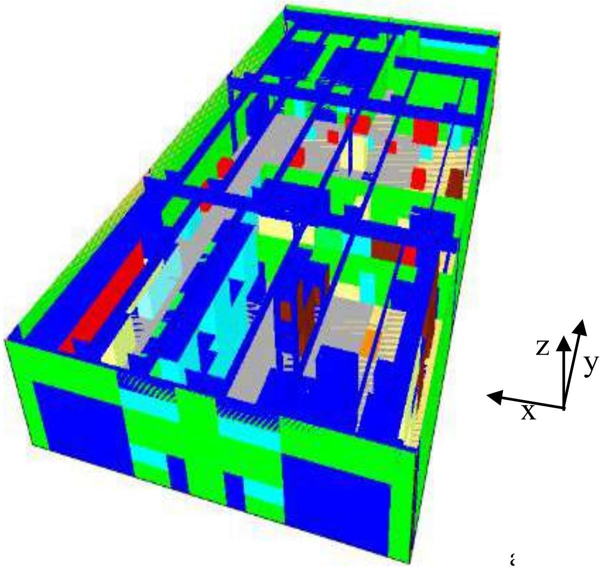

Figure 7. CFD model of the fire zone

In the numerical model, the compartment boundaries were assumed to be adiabatic; however, special attention was devoted to the modeling of the openings, as discussed in a later section. The computational mesh comprises 4,800 predominantly cubic cells (dimensions: 1.02 × 1.00 × 1.13 m). A time step of 1 millisecond (10^{-3} s) was selected based on a convergence study conducted across various time steps, ensuring numerical stability and accuracy with the chosen mesh.

The initial (pre-incident) conditions include an ambient temperature of 20 °C, an oxygen concentration of 20.70% by volume, and standard atmospheric pressure (1 atm or 101,325 Pa). The compartment is neither served by a mechanical ventilation system, nor is it equipped with fire detection or automatic fire suppression systems.

The materials present in the domain, along with their key thermophysical properties, are summarized in Table 4.

Please cite this document as: Stochino, F., Majumder, A., Kanagaraj, B., Sara, N., Serra, A., & Mistretta, F. (2025). Combining experimental and computational approaches for post-fire safety assessment of RC warehouse. *Proceedings of the Institution of Civil Engineers-Forensic Engineering*, *178*(3), 66-*80*. *https://doi.org/10.1680/jfoen.25.00027*

Table 4. Various materials and their burning characteristics.

Material Category	**Density (kg/m³)**	**Thickness (m)**	**Thermal Conductivity (W/m·K)**	**Specific Heat Capacity (kJ/kg·K)**	**Heat Release Rate per Unit Area (kW/m²)**	**Ignition Threshold (°C)**
Textiles (Clothes)	561	0.025	0.113	0.518	391.4	296
Synthetic Rubber (SBR)	1100	0.02	0.17	1.88	1980.97	390
Cellulose (Paper)	930	0.007	0.18	1.34	1.561	230
Thermoplastic (PP)	900	0.006	0.38	6.3	1782.44	210
Polymer Blend (PE-PP)	915	0.008	0.38	3.45	273	309
Construction (Drywall)	800	0.013	0.2	8	408	230
Metal (Steel)	7900	0.01	14.9	0.477	131.91	400
Storage (Shelving)	7900	0.007	0.14	0.471	255.44	400
Electrical (Panel)	8920	0.123	390	0.385	429.775	300
Composite (Steel + Paper)	2324	0.017	14.9	0.477	432.811	230
Composite (Steel + Plastic)	2312	0.017	14.9	0.477	55.697	210
Packaging (PET Pallets)	600	0.1	0.12	2.72	3811.294	210

Although the precise origin and cause of the fire remain uncertain, it is suspected that a short circuit in the lift truck's electrical system—located beneath beam T4 (refer to Figs. 2b and 5a)—may have triggered the ignition. The Heat Release Rate Per Unit Area (HRRPUA) for this item was taken from (Särdqvist, 1993) and is shown in *Figure 8*.

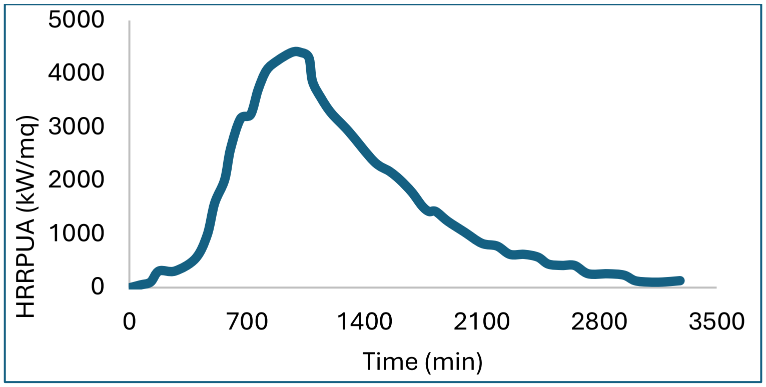

Figure 8. HRRPUA curve.

Please cite this document as: Stochino, F., Majumder, A., Kanagaraj, B., Sara, N., Serra, A., & Mistretta, F. (2025). Combining experimental and computational approaches for post-fire safety assessment of RC warehouse. *Proceedings of the Institution of Civil Engineers-Forensic Engineering*, *178*(3), 66-*80*. *https://doi.org/10.1680/jfoen.25.00027*

As the fire spread to additional combustible materials in the compartment, their contributions to the overall heat release were modeled using the parameters provided in Table 4.

The fire brigade arrived on scene and managed to suppress the fire. During their intervention, they forcibly opened two doors at the lower part of the building (see Fig. 2), which was modeled as occurring at t = 1,200 seconds (20 minutes). As interior conditions deteriorated, making direct access unsafe, one rolling shutter was subsequently opened to allow for external hose streams. This action was simulated at t = 5,400 seconds (90 minutes). However, access to the shutter was hindered by wood pallets stacked up to the ceiling and placed directly in front of the opening. Consequently, it was decided to open a series of windows located on the opposite side of the hall at a height of 4.45 m on the upper side of the plant in Fig. 2 at t = 6,000 seconds (100 minutes). To monitor the thermal evolution within the compartment, 78 thermocouples were modeled. Their spatial arrangement formed an approximate 5×5 m mesh, with sensors positioned at various heights on the sides of beams and columns. The average temperatures recorded are depicted in *Figure 9*.

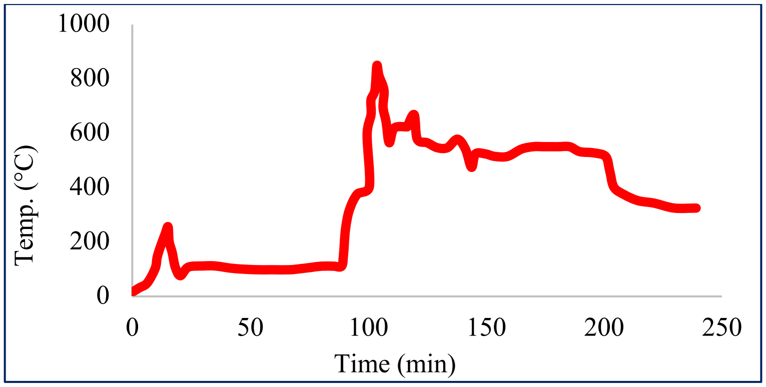

Figure 9. The average temperature-time diagram (CFD model).

A notable increase in temperature is observed following the window openings at 100 minutes, likely due to the influx of oxygen enhancing combustion.
Development of fire within the CFD simulation is visualized in
Figure 10, where flame propagation is clearly illustrated.

Please cite this document as: Stochino, F., Majumder, A., Kanagaraj, B., Sara, N., Serra, A., & Mistretta, F. (2025). Combining experimental and computational approaches for post-fire safety assessment of RC warehouse. *Proceedings of the Institution of Civil Engineers-Forensic Engineering*, *178*(3), 66-*80*. *https://doi.org/10.1680/jfoen.25.00027*

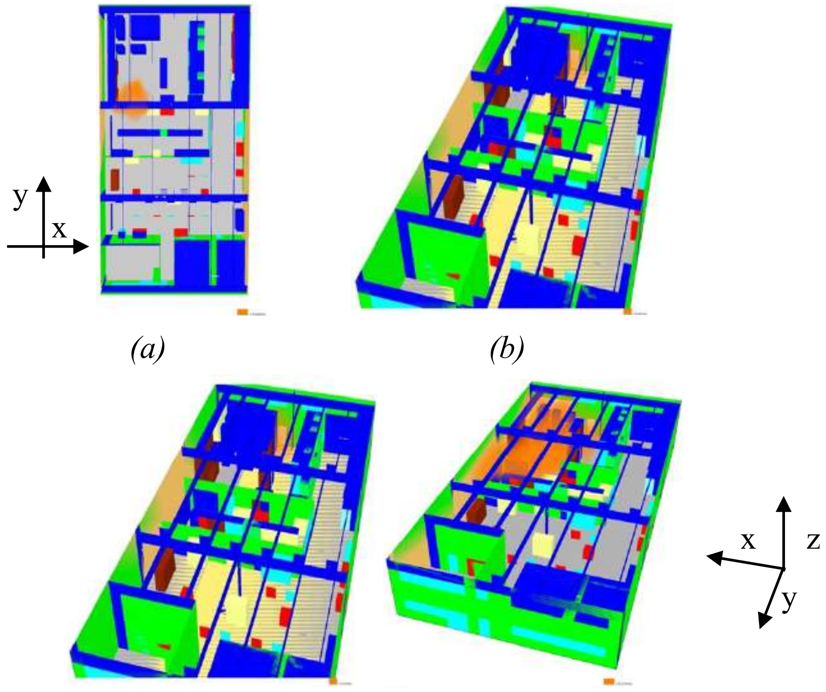

(a) (b)

(c) (d)

Figure 10. CFD model of the fire developing in the compartment at (a) t=15 mins, (b) t=25 mins, (c) t=90 mins, and (d) t=1000 mins.

Table 5 presents a comparison between the maximum temperatures predicted by the numerical model and those derived from microstructural and colorimetric analyses (considered benchmarks, see Table 2 and Table 4). The simulation results demonstrate good agreement with experimental data, exhibiting an average error of 15%. Given the complexity of the scenario and the number of unknown parameters, this level of accuracy is considered satisfactory.

Table 5. A comparative analysis of the maximum temperatures forecasted by the numerical model.

Column number	**Height (m)**	**Exp. Max Temp (°C)**	**CFD Max Temp (°C)**	**Difference (%)**
5 b	4.73	>500	613	22%
5 a	1.06	500	722	44%
7	1.55	500	532	6%
9 a	4.36	500	506	1%
9 b	0.98	500	384	23%

Beam number	**Height (m)**	**Exp. Max Temp (°C)**	**CFD Max Temp (°C)**	**Difference (%)**
5–6	5.9	830–860	801	5%
8–9	5.9	500	565	13%
9–10	6.7	820–920	836	4%

Please cite this document as: Stochino, F., Majumder, A., Kanagaraj, B., Sara, N., Serra, A., & Mistretta, F. (2025). Combining experimental and computational approaches for post-fire safety assessment of RC warehouse. *Proceedings of the Institution of Civil Engineers-Forensic Engineering*, *178*(3), 66-*80*. *https://doi.org/10.1680/jfoen.25.00027*

4.3. Columns

The temperature data recorded by the thermocouples were used as input for a thermomechanical analysis conducted using SAFIR (Franssen, 2005). This approach allowed for the investigation of both the temperature distribution within the cross-section of the structural elements and their mechanical response under fire conditions. In this study, the nonlinear constitutive behavior of concrete and steel has been modeled in accordance with the provisions of EN 1992-1-1 (“EN 1992-1-1”, n.d.).

For example, for Column 5 which was exposed to fire on all sides the maximum temperature distribution obtained from the FE thermal simulation was compared with estimates derived from the post-fire in-situ investigation (see Tables 2 and 4). The field tests made it possible to estimate the maximum temperatures reached at various depths from the column’s external surface.

Figure 11 illustrates finite element temperature distribution across the cross-section of Column 5 at a height of 4.45 m, compared with the estimated maximum in-situ temperature. It shows that the surface temperature of Column 5 reached approximately 600 °C, while at a depth of 4 cm from the surface, the maximum temperature was around 300 °C. The variations in temperature across different sides of the column can be attributed to the temperature time-history produced by the CFD (Computational Fluid Dynamics) fire simulation. Since the fire scenario was not symmetrical, the resulting temperature distribution is inherently non-uniform.

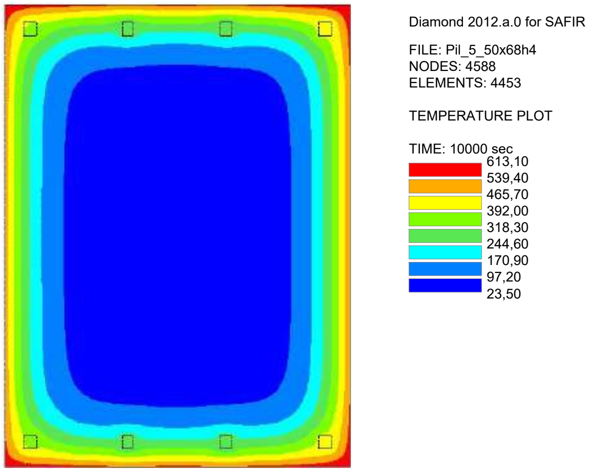

Figure 11. Finite element temperature distribution in the cross-section of Column 5.

4.4. Beams

Figure 12 illustrates the maximum temperature distribution and the deflection-time history of beam T5 (see, Figure 6), which was modeled using 32 beam elements. The varying temperature fields derived from the CFD analysis lead to different thermo-mechanical responses in each section of the beam. The beam is directly exposed to fire on its underside and lateral faces, while the ceiling slab shields the top surface. As shown in Figure 12, the highest temperature, 483 °C, occurs at the bottom of the beam.

Please cite this document as: Stochino, F., Majumder, A., Kanagaraj, B., Sara, N., Serra, A., & Mistretta, F. (2025). Combining experimental and computational approaches for post-fire safety assessment of RC warehouse. *Proceedings of the Institution of Civil Engineers-Forensic Engineering*, *178*(3), 66-*80*. *https://doi.org/10.1680/jfoen.25.00027*

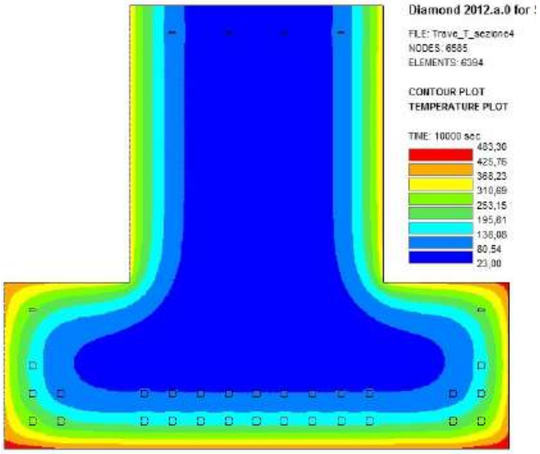

Figure 12. Max. temperature distribution of beam T5 midspan cross section;

4.5. Nonlinear Transient Thermal Analysis of Column 6

Specific attention is necessary for the lateral column 6. This rectangular column (90x60 cm) is characterized by the presence of an internal rainwater downpipe that channels roof runoff to the sewer system. The water contained within the downpipe likely underwent significant thermal expansion due to the fire, contributing to the spalling of a large portion of the concrete within the fire-exposed region of the column, see Figure 13.

Figure 13. Column 6 damages.

A nonlinear thermomechanical coupled analysis has been developed in ANSYS to describe this phenomenon. The input temperatures were obtained by the CFD analysis presented in Section 4.3. Figure 14 shows the color scale distribution of temperatures at the various loading steps. At 455 s,

Please cite this document as: Stochino, F., Majumder, A., Kanagaraj, B., Sara, N., Serra, A., & Mistretta, F. (2025). Combining experimental and computational approaches for post-fire safety assessment of RC warehouse. *Proceedings of the Institution of Civil Engineers-Forensic Engineering*, *178*(3), 66-*80*. *https://doi.org/10.1680/jfoen.25.00027*

heat is concentrated near the lower boundary with minimal spread. By 6415 s, heat started propagating upward. At 10,000 s, the structure shows widespread heating, with the highest temperatures near the heat source.

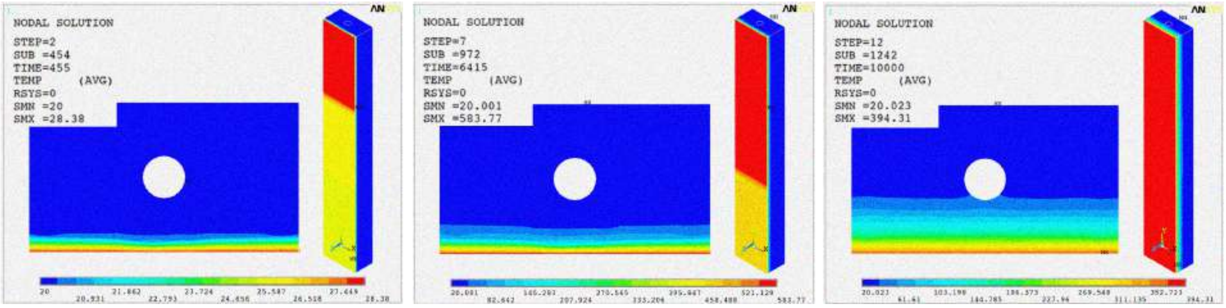

(a) *(b)* *(c)*

Figure 14. Temperature distribution at (a) t = 455s, (b) t=6415s, and (c) t=10000s

From Figure 15, it is possible to observe how the column deforms in response to the applied thermal and structural loads. Initially, the deformation of the column is due solely to the structural load. As the temperature increases, thermal stress becomes more significant, leading to a noticeable change in the deformed shape.

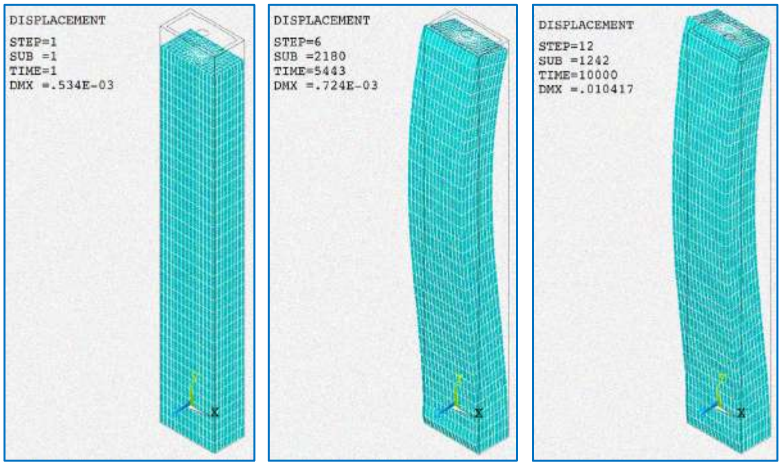

(a) *(b)* *(c)*

Figure 15. Deformation at (a) t = 1s, (b) t=5443s, and (c) t=10000s.

Figure 16 (a, b, and c) presents the time-dependent displacement along the Y-axis of a column under dynamic loading, captured at three different selected times (t=1s, t=3263s, and t=10000s). The color gradient represents the blue (lower displacement) to red (higher displacement), visually depicting the variation in displacement intensity, with red zones consistently indicating regions of maximum response.

Please cite this document as: Stochino, F., Majumder, A., Kanagaraj, B., Sara, N., Serra, A., & Mistretta, F. (2025). Combining experimental and computational approaches for post-fire safety assessment of RC warehouse. *Proceedings of the Institution of Civil Engineers-Forensic Engineering*, *178*(3), 66-*80*. https://doi.org/10.1680/jfoen.25.00027

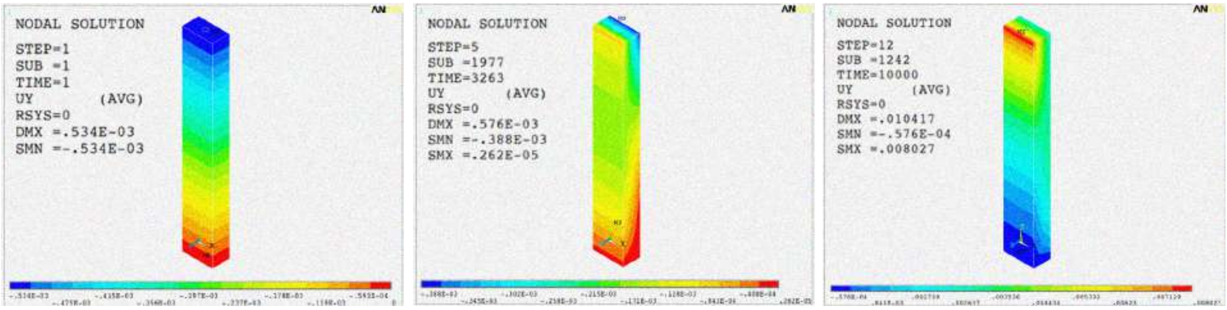

(a) (b) (c)

Figure 16. Displacement in the y-direction at (a) t = 1s, (b) t = 3263s, and (c) t = 10000s.

Figure *17* (a, b, and c) presents the time-dependent displacement along the Z-axis of a column under dynamic loading, captured at three different selected times (t=1s, t=6415s, and t=10000s). The color gradient represents the blue (lower displacement) to red (higher displacement), visually depicting the variation in displacement intensity, with red zones consistently indicating regions of maximum response.

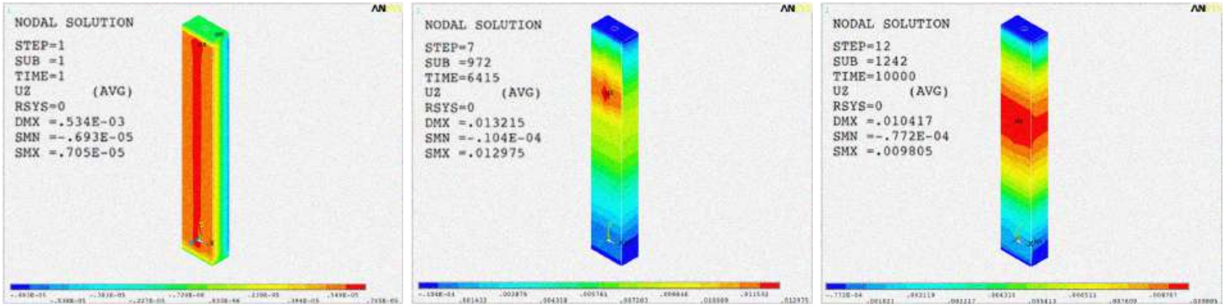

(a) (b) (c)

Figure 17. Displacement in the z-direction at (a) t = 1s, (b) t = 6415s, and (c) t = 10000s.

Figure 18 (a, b, and c) shows the first principal stress (at t = 1s, t = 5443s, and *t* = 10000*s)*, and Figure 19 (a, b, and c) shows the second principal stress (at t = 1s, t = 6541s, and *t* = 10000*s)*. Notably, these are useful for understanding the distribution of stress on the faces of the column. Principal stresses indicate maximum stress, helping identify critical zones where failure may occur.

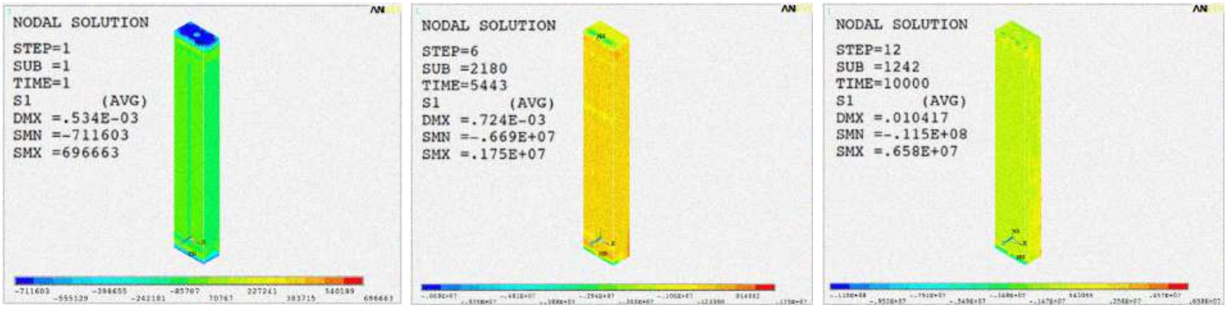

Please cite this document as: Stochino, F., Majumder, A., Kanagaraj, B., Sara, N., Serra, A., & Mistretta, F. (2025). Combining experimental and computational approaches for post-fire safety assessment of RC warehouse. *Proceedings of the Institution of Civil Engineers-Forensic Engineering*, *178*(3), 66-*80*. *https://doi.org/10.1680/jfoen.25.00027*

(a) (b) (c)

Figure 18. First principal stress at (a) t = 1s, (b) t = 5443s, and (c) t =10000s.

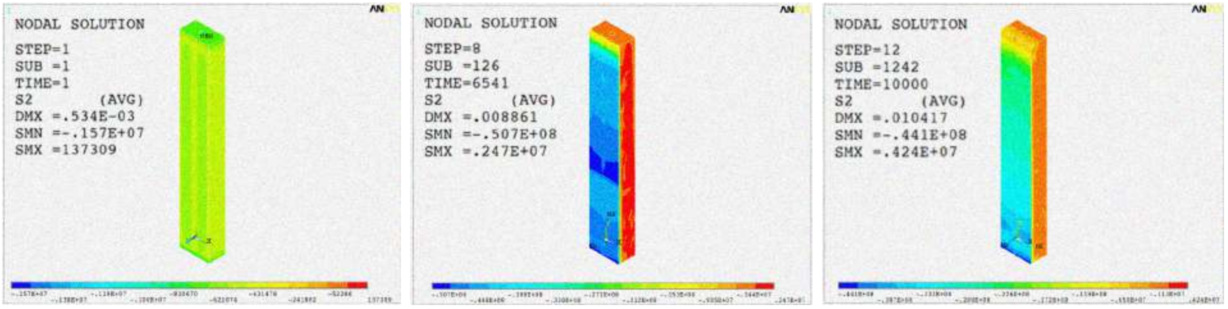

(a) (b) (c)

Figure 19. Second principal stress at (a) t = 1s, (b) t = 6541s, and (c) t = 10000s.

Figure 20 (a, b, and c) presents the first principal stress (at t = 1s, t = 5443s, and *t* = 10000*s)*. These are useful for understanding the distribution of stresses on the faces of the column. Principal stresses indicate maximum stresses, helping identify critical zones where failure may occur.

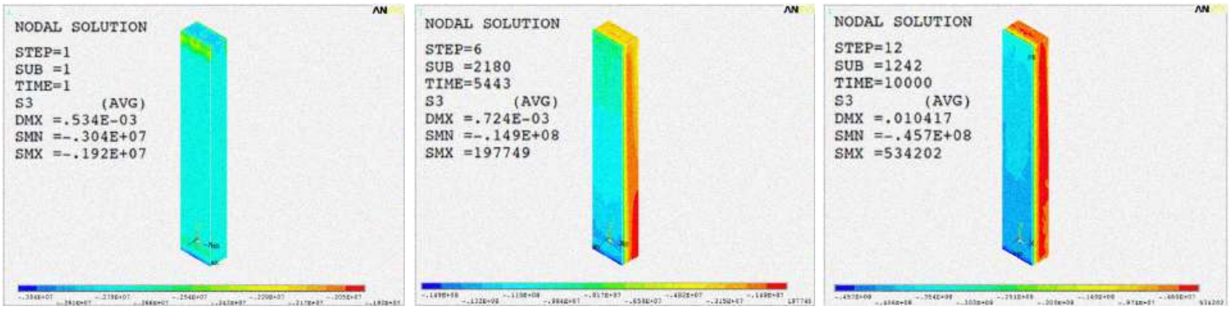

(a) (b) (c)

Figure 20. Third principal stress at (a) t = 1s, (b) t = 5443s, and (c) t = 10000s.

Figure 21(a) illustrates the damage state at 6880 seconds; at this moment, the entire surface affected by the fire exhibits the highest temperatures. Figure 21(b) shows a comparison between the real image of the damaged column and the results obtained through computational mechanics.

Please cite this document as: Stochino, F., Majumder, A., Kanagaraj, B., Sara, N., Serra, A., & Mistretta, F. (2025). Combining experimental and computational approaches for post-fire safety assessment of RC warehouse. *Proceedings of the Institution of Civil Engineers-Forensic Engineering*, *178*(3), 66-*80*. *https://doi.org/10.1680/jfoen.25.00027*

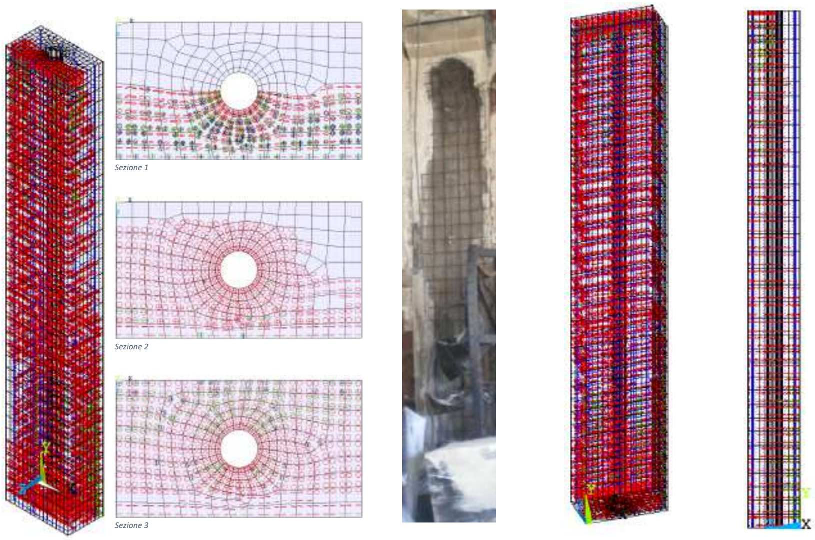

(a) (b)

Figure 21. (a) Damage at 6880 sec, and (b) Comparison of the damage.

5. Conclusion

This study has proved the effectiveness of an integrated approach combining advanced experimental diagnostics with high-fidelity CFD and FE modeling for post-fire assessment of RC structures. The analysis of a fire-damaged warehouse revealed significant degradation in structural elements, particularly columns and prestressed beams, due to asymmetric thermal exposure and internal factors such as embedded downpipes. Non-destructive tests and microstructural analyses provided reliable benchmarks for temperature estimation, validating the numerical simulations. The coupled methodology not only enhanced understanding of the fire-induced damage mechanisms but also offered a robust framework for evaluating residual capacity and planning retrofitting interventions.

Thermal restraint played a critical role in the observed damage patterns and residual behavior of the structural elements. The beams, which were partially shielded by the slab and fixed at their supports, experienced restricted thermal expansion, generating additional axial forces and bending moments that exacerbated concrete spalling and tendon exposure. Similarly, columns subjected to asymmetric heating exhibited thermal gradients across their sections, while surrounding framing elements limited lateral expansion. This restraint induced secondary stresses and curvature that accelerated material degradation and stiffness loss. These findings highlight that thermal restraint, often overlooked in simplified analyses, significantly influences the overall fire response and must be considered to achieve accurate post-fire safety assessments and reliable retrofitting strategies.

In conclusion, this paper contributes to performance-based fire engineering practices by demonstrating a robust and integrated methodology that combines detailed experimental diagnostics, advanced computational modeling, and material characterization. The findings offer deeper insights into the thermal and mechanical behavior of fire-damaged reinforced concrete structures, emphasizing the need to account for thermal restraint and fire-induced degradation in

Please cite this document as: Stochino, F., Majumder, A., Kanagaraj, B., Sara, N., Serra, A., & Mistretta, F. (2025). Combining experimental and computational approaches for post-fire safety assessment of RC warehouse. *Proceedings of the Institution of Civil Engineers-Forensic Engineering*, *178*(3), 66-*80*. *https://doi.org/10.1680/jfoen.25.00027*

post-fire assessments. This knowledge supports more informed decision-making processes, enabling engineers to evaluate structural integrity more reliably and to design targeted, cost-effective interventions. Ultimately, this approach promotes safer and more resilient reconstruction strategies, enhances the sustainability of repair measures, and provides a practical foundation for future research and engineering guidelines focused on improving the fire performance of similar structural systems.

References

Bolina, F.L. and Rodrigues, J.P.C. (2022), “Numerical study and proposal of new design equations for steel decking concrete slabs subjected to fire”, *Engineering Structures*, Vol. 253, p. 113828, doi: 10.1016/j.engstruct.2021.113828.

Çelik, Z. and Urtekin, Y. (2025), “Effects of High Temperature and Water Re-Curing on the Flexural Behavior and Mechanical Properties of Steel–Basalt Hybrid Fiber-Reinforced Concrete”, *Applied Sciences*, Vol. 15 No. 3, p. 1587, doi: 10.3390/app15031587.

Chen, Y., Wang, Y., Song, A. and Zhao, L. (2024), “Effects of High-Temperature Environments on the Thermodynamic Performance of Reinforced Concrete Bridge Structures”, *International Journal of Heat and Technology*, Vol. 42 No. 5, pp. 1541–1550, doi: 10.18280/ijht.420507.

Chorin, A.J. (1968), “Numerical solution of the Navier-Stokes equations”, *Mathematics of Computation*, Vol. 22 No. 104, pp. 745–762, doi: 10.1090/S0025-5718-1968-0242392-2.

“EN 1992-1-1”. (n.d.). .

Franssen, J.-M. (2005), “SAFIR: A Thermal and Structural Program for Modeling Structures Under Fire”, *Engineering Journal*, Vol. 42 No. 3, pp. 143–158, doi: 10.62913/engj.v42i3.856.

Gernay, T. (2024), “Performance-based design for structures in fire: Advances, challenges, and perspectives”, *Fire Safety Journal*, Vol. 142, p. 104036, doi: 10.1016/j.firesaf.2023.104036.

Jiao, Y., Liu, H., Wang, X., Zhang, Y., Luo, G. and Gong, Y. (2014), “Temperature Effect on Mechanical Properties and Damage Identification of Concrete Structure”, *Advances in Materials Science and Engineering*, Vol. 2014, pp. 1–10, doi: 10.1155/2014/191360.

Khan, A.A., Usmani, A. and Torero, J.L. (2021), “Evolution of fire models for estimating structural fire-resistance”, *Fire Safety Journal*, Vol. 124, p. 103367, doi: 10.1016/j.firesaf.2021.103367.

La Scala, A., Loprieno, P., Foti, D. and La Scala, M. (2023), “The Mechanical Response of Structural Elements in Enclosed Structures during Electric Vehicle Fires: A Computational Study”, *Energies*, Vol. 16 No. 21, p. 7233, doi: 10.3390/en16217233.

La Scala, A., Loprieno, P., Ivorra, S., Foti, D. and La Scala, M. (2024), “Modal Analysis of a Fire-Damaged Masonry Vault”, *Fire*, Vol. 7 No. 6, p. 194, doi: 10.3390/fire7060194.

La Scala, A., Śliwa-Wieczorek, K., Rizzo, F., Sabbà, M.F. and Zając, B. (2024), “Flexible Polyurethane Adhesives: Predictive Numerical Model Calibration through Experimental Testing at Elevated Temperature”, *Applied Sciences*, Vol. 14 No. 5, p. 1943, doi: 10.3390/app14051943.

Li, M., Qian, C. and Sun, W. (2004), “Mechanical properties of high-strength concrete after fire”, *Cement and Concrete Research*, Vol. 34 No. 6, pp. 1001–1005, doi: 10.1016/j.cemconres.2003.11.007.

Ma, C., Du, H., Luan, S., Dong, E., Gardner, L.M. and Gernay, T. (2025), "From Occurrence to Consequence: A Comprehensive Data-driven Analysis of Building Fire Risk", arXiv, doi: 10.48550/ARXIV.2503.22689.

Maragkos, G. and Beji, T. (2021), "Review of Convective Heat Transfer Modelling in CFD Simulations of Fire-Driven Flows", *Applied Sciences*, Vol. 11 No. 11, p. 5240, doi: 10.3390/app11115240.

McGrattan, K. and Miles, S. (2016), "Modeling Fires Using Computational Fluid Dynamics (CFD)", in Hurley, M.J., Gottuk, D., Hall, J.R., Harada, K., Kuligowski, E., Puchovsky, M., Torero, J., et al. (Eds.), *SFPE Handbook of Fire Protection Engineering*, Springer New York, New York, NY, pp. 1034–1065, doi: 10.1007/978-1-4939-2565-0_32.

McGrattan, K.B. (2006), *Fire Dynamics Simulator (Version 4) : Technical Reference Guide*, No. NIST SP 1018, 0 ed., National Institute of Standards and Technology, Gaithersburg, MD, p. NIST SP 1018, doi: 10.6028/NIST.SP.1018.

Meloni, P., Mistretta, F., Stochino, F. and Carcangiu, G. (2019), "Thermal Path Reconstruction for Reinforced Concrete Under Fire", *Fire Technology*, Vol. 55 No. 5, pp. 1451–1475, doi: 10.1007/s10694-019-00835-7.

Osman, M.H., Sarbini, N.N., Ibrahim, I.S., Ma, C.K., Ismail, M. and Mohd, M.F. (2017), "A case study on the structural assessment of fire damaged building", *IOP Conference Series: Materials Science and Engineering*, Vol. 271, p. 012100, doi: 10.1088/1757-899X/271/1/012100.

Pinna, F. and Stochino, F. (2025), "Nonlinear SDOF model for dynamic response and fragility analysis of steel plates under blast loads", *European Journal of Environmental and Civil Engineering*, pp. 1–24, doi: 10.1080/19648189.2025.2508209.

Please cite this document as: Stochino, F., Majumder, A., Kanagaraj, B., Sara, N., Serra, A., & Mistretta, F. (2025). Combining experimental and computational approaches for post-fire safety assessment of RC warehouse. *Proceedings of the Institution of Civil Engineers-Forensic Engineering*, *178*(3), 66-*80*. *https://doi.org/10.1680/jfoen.25.00027*

Pinna, F., Zucca, M., Simoncelli, M. and Stochino, F. (2025), "Explosion Venting in Dust Collectors: A Critical Review of Standards for Reduced Pressure and Reaction Force Duration", *Journal of Loss Prevention in the Process Industries*, p. 105670, doi: 10.1016/j.jlp.2025.105670.

Qin, D., Gao, P., Aslam, F., Sufian, M. and Alabduljabbar, H. (2022), "A comprehensive review on fire damage assessment of reinforced concrete structures", *Case Studies in Construction Materials*, Vol. 16, p. e00843, doi: 10.1016/j.cscm.2021.e00843.

Raposo, J.R.N., Raposo, H.D.N., Reis, L., Almeida, E. and Rodrigues, A. (2025), "Fire in house: investigation of the outbreak and spread of the fire in a countryside house", *Proceedings of the Institution of Civil Engineers - Forensic Engineering*, Vol. 178 No. 1–2, pp. 1–7, doi: 10.1680/jfoen.24.00007.

Saeed, M.H. and Al-Ahmed, A.H.A. (2025), "Behavior and Strength Prediction of Concrete Beams reinforced with GFRP Bars and subjected to High Temperature", *Engineering, Technology & Applied Science Research*, Vol. 15 No. 1, pp. 19848–19855, doi: 10.48084/etasr.9454.

Särdqvist, S. (1993), *Initial Fire. RHR, Smoke Production and CO Generation from Single Items and Room Fire Tests*, No. ISRN LUTVDG/TVBB--3070—SE, Lund.

Stochino, F. (2016), "RC beams under blast load: Reliability and sensitivity analysis", *Engineering Failure Analysis*, Vol. 66, pp. 544–565, doi: 10.1016/j.engfailanal.2016.05.003.

Stochino, F., Mistretta, F., Meloni, P. and Carcangiu, G. (2017a), "Integrated Approach for Post-fire Reinforced Concrete Structures Assessment", *Periodica Polytechnica Civil Engineering*, doi: 10.3311/PPci.9830.

Stochino, F., Mistretta, F., Meloni, P. and Carcangiu, G. (2017b), “Integrated Approach for Post-fire Reinforced Concrete Structures Assessment”, *Periodica Polytechnica Civil Engineering*, doi: 10.3311/PPci.9830.

Wen, J.X. (2024), “Fire modelling: The success, the challenges, and the dilemma from a modeller’s perspective”, *Fire Safety Journal*, Vol. 144, p. 104087, doi: 10.1016/j.firesaf.2023.104087.

Yan, Z., Zhou, Z., Shen, Y., Li, J., Guan, L. and Zhu, H. (2024), “Structural fire investigation and analysis on rectangular shield tunnel assembled by composite segments”, *Engineering Failure Analysis*, Vol. 158, p. 107966, doi: 10.1016/j.engfailanal.2024.107966.

Please cite this document as: Stochino, F., Majumder, A., Kanagaraj, B., Sara, N., Serra, A., & Mistretta, F. (2025). Combining experimental and computational approaches for post-fire safety assessment of RC warehouse. *Proceedings of the Institution of Civil Engineers-Forensic Engineering*, *178*(3), 66-*80*. *https://doi.org/10.1680/jfoen.25.00027*